Anisotropic Motion and Molecular Dynamics of Cholesterol, Lanosterol, and Ergosterol in Lecithin Bilayers Studied by Quasi-elastic Neutron Scattering†

Emil Endress,‡ Helmut Heller,§ Hélène Casalta,|| Michael F. Brown,⊥ and Thomas M. Bayerl*,‡

Physikalisches Institut EP5, Universität Würzburg, D-97074 Würzburg, Germany, Leibniz Rechenzentrum, München, Germany, Institut Laue-Langevin, Grenoble, France, and Department of Chemistry, University of Arizona, Tucson, Arizona 85721

Received March 5, 2002; Revised Manuscript Received June 27, 2002

ABSTRACT: Quasi-elastic neutron scattering (QENS) was employed to study the molecular dynamics of three structurally related sterols, namely, cholesterol, lanosterol, and ergosterol. Oriented bilayers of dipalmitoylphosphatidylcholine (DPPC) were investigated at 40 mol % sterol content and at three temperatures (20, 36, and 50 °C) for two energy resolutions. Data analysis was concentrated on a direct comparison of the out-of-plane and the in-plane high-frequency motions of the three sterols in terms of their rates and amplitudes. The (spatially restricted) diffusive motion of the three sterols in the two directions was characterized by diffusion constants in the range of $(5-30) \times 10^{-12}$ m^2 s^{-1}, with a significantly faster rate of diffusion along the membrane normal, resulting in a diffusional anisotropy, D_a. At low temperature (20 °C), cholesterol showed the highest value ($D_a = 4.5$), while lanosterol gave the lowest one ($D_a = 2.0$). At high temperature (50 °C), ergosterol diffusion had the highest diffusion anisotropy ($D_a = 2.0$) compared to lanosterol ($D_a = 1.8$) and cholesterol ($D_a = 1.6$). Most interestingly, cholesterol showed at all three temperatures an amplitude of its out-of-plane-motion of 1.0−1.1 nm, more than a factor of 3 higher than measured for the other two sterols. This finding suggests that the short alkyl chain of the cholesterol molecule may cross at high frequency the bilayer midplane, while the other two sterols remain confined within the geometrical limits of each monolayer leaflet. The results provide an example of how slight structural alterations of sterols can affect their molecular dynamics in bilayers, which in turn may be relevant to the membrane micromechanical properties.

Cholesterol, the dominant sterol constituent of eukaryotic cell membranes, has been studied in mixtures with lipids by a wide variety of methods [cf. (*1*) and references cited therein]. Recently, the role of cholesterol in membrane lipid rafts has attracted interest, which are proposed to comprise discrete microdomains of sphingolipids and cholesterol, together with glycosylphosphatidylinositol (GPI)-anchored membrane proteins (*2*−*5*). Besides its unique phase behavior (*6*−*9*) in mixtures with lecithin, and the well-established modulation of membrane micromechanical properties and dynamics (*10*−*14*), cholesterol exhibits an interesting anisotropy of motion within the bilayer on the molecular dynamics time scale. In a recent quasi-elastic neutron scattering (QENS)[1] study, we observed this anisotropy in the gigahertz frequency range at physiological temperature in synthetic lecithin (dipalmitoylphosphatidylcholine, DPPC) bilayers at 40 mol % cholesterol content (*15*). A salient feature of this anisotropy was a fast (confined) diffusion of the sterol over distances of more than 1 nm parallel to the membrane normal (throughout the text, motions parallel to the membrane normal are denoted as out-of-plane or transverse motions, motions parallel to the membrane plane as in-plane or lateral motions). This rather large amplitude of transverse motion [for comparison, lecithin exhibits an out-of-plane motion of less than 0.2 nm (*16*)] suggested that part of the cholesterol molecule such as its short alkyl chain can fluctuate at high frequencies into the opposite monolayer leaflet. In a time-averaged picture, this would correspond to a dynamic roughness at the bilayer midplane (or to a dynamic interdigitation of the two monolayers), rendering the frictional drag between the monolayers significantly higher than in a cholesterol-free fluid bilayer. This effect might contribute to the above-mentioned increase of membrane bending energy by cholesterol, and to the unique phase behavior of cholesterol/lecithin mixtures (*6*, *7*, *9*, *14*, *17*).

During the evolution of cells and membranes, other sterols beside cholesterol have gained some importance, most noteworthy lanosterol (the evolutionary precursor of cholesterol) but also ergosterol. Lanosterol represents the major sterol constituent of prokaryotic cell membranes, while ergosterol occurs in the membranes of certain protozoa, yeast, and other fungi (*18*). An intriguing question is now whether

† This work was supported by grants from the Deutsche Forschungsgesellschaft, the BMBF, and the NIH. M.F.B. was supported by the Röntgen-Professorship award of the Volkswagen Stiftung at the Department of Physics of the University of Würzburg.

* Correspondence should be addressed to this author at the Universität Würzburg, Physikalisches Institut EP5, Am Hubland, D-97074 Würzburg, Germany.

‡ Universität Würzburg.

§ Leibniz Rechenzentrum.

|| Institut Laue-Langevin.

⊥ University of Arizona.

[1] Abbreviations: QENS, quasi-elastic neutron scattering; QISF, quasi-elastic incoherent structure factor; EISF, elastic incoherent structure factor; DBF, detailed balance factor; DWF, Debye−Waller factor; DPPC, dipalmitoylphosphatidylcholine; FWHM, full width at half-maximum.

10.1021/bi0201670 CCC: $22.00
Published on Web 10/04/2002

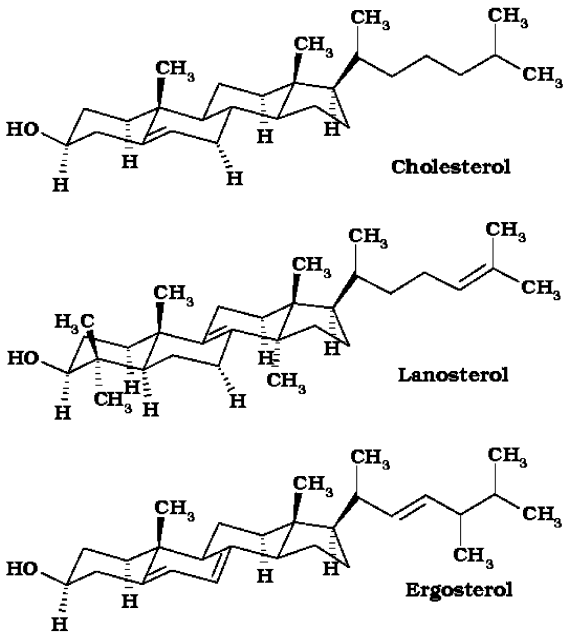

FIGURE 1: Molecular structures of cholesterol, lanosterol, and ergosterol.

the slight structural differences of these two sterols compared to cholesterol (cf. Figure 1) may result—under otherwise identical conditions—in differences of their molecular dynamics in lecithin bilayers. To address this problem, we employed quasi-elastic neutron scattering (QENS) in a direct comparison of DPPC bilayers containing 40 mol % of either cholesterol, lanosterol, or ergosterol. Since QENS is a method which can simultaneously measure spatial and temporal correlations of molecular motion, the comparison can be expected to shed some light on the possible connection between sterol structure and its molecular dynamics, and how such molecular properties may contribute to microscopic or even macroscopic function.

MATERIALS AND METHODS

Materials and Sample Preparation. Deuterated 1,2-dipalmitoyl-d_{31}-glycero-*sn*-3-phosphocholine-d_{13} (DPPC-d_{75}) was purchased from Avanti Polar Lipids (Alabaster, AL), and all sterols were obtained from Fluka (Neu-Ulm, Germany). Highly purified D_2O was obtained from Deuchem (Leipzig, Germany). Solid substrates for multilayer preparation were highly polished, undoped silicon wafers (Applications Couches Minces, France) of 150 μm thickness, 3 × 5 cm area, and surface roughness of less than 1 Å as measured by atomic force microscopy.

Oriented multilayers of DPPC-d_{75} containing 40 mol % of sterol were prepared according to procedures described in detail previously (*16*). About 1000 bilayers were sandwiched between 2 wafers with 10 wafers per sample, i.e., a total of about 9000 bilayers. This bilayer mass corresponded to about 500 mg of total weight of lipid and sterol in the sample. Hydration was adjusted after annealing the samples for 12 h at 90 °C in D_2O vapor at 20 wt % D_2O. The final oriented samples showed a mosaic spread of less than 2° upon examination by X-ray diffraction (*16*).

Method. Since QENS is a method that is not commonly used in biophysics, a few basic features of dynamic neutron scattering should be recalled here. The neutron as a spin-1/2 particle can be scattered with and without spin flip. As a result, two scattering cross sections have to be distinguished, giving rise to coherent and incoherent scattering. The former probes the pair-correlation function between different scatterers in a sample, and thus provides both structural information and correlated dynamics. By contrast, incoherent scattering probes the autocorrelation function of the individual scattering particles, i.e., the molecular dynamics of the molecules. The possibility of distinguishing the two cross sections makes neutron scattering a unique tool for the investigation of membrane dynamics. A deliberate distinction between the two types of scattering is possible by simply choosing a "convenient" scatterer in the sample. For biological applications, the most important incoherent scatterer is the hydrogen atom. Deuterium scatters mainly coherently but much more weakly than the incoherent scattering of the proton. Thus, (selective) deuteration offers a means to mask (parts of) the molecules in incoherent scattering experiments. In our case, the DPPC-d_{75} was nearly fully deuterated along with the hydration water (D_2O) to observe the incoherent scattering arising mainly from the (nondeuterated) sterols. Since the motional and phase transition behavior of the lipids is drastically influenced by the presence of the sterol, the measurement of pure DPPC-d_{75} in D_2O and its subtraction from the sterol−DPPC-d_{75} spectra is not a valid procedure for coherent and incoherent background elimination. This approach would require a fully deuterated sterol as well, which is not available. However, since the incoherent signal from the deuterated lipid and the D_2O contributes to the total signal only by less than 10%, this contribution was neglected. Similarly, the coherent scattering can lead to a high intensity at a q value of about 2.0 Å^{-1}, but below 1.6 Å^{-1} incoherent scattering dominates strongly the signal (*19*).

The time scale at which the correlation functions are probed is determined by the energy resolution Γ of the spectrometer. By employing various energy resolutions, different time domains of the correlation function can be probed selectively. Fourier transformation in space and time of the measured correlation function leads to the dynamic structure factor $S(\boldsymbol{q},\omega)$. Here $\boldsymbol{q}$ is the momentum transfer and ω the frequency. For data analysis, $S(\boldsymbol{q},\omega)$ can be separated into the elastic incoherent structure factor (EISF, having a line shape which depends on the resolution function of the instrument) and the quasi-elastic incoherent structure factor (QISF, which has a Lorentzian line shape for all models considered in the present application). The EISF is solely a function of $\boldsymbol{q}$ and describes the structure and spatial extent of the molecular motion, whereas the QISF is a Lorentzian function of ω and contains information about the motional rates and dynamics.

Generally, the total incoherent structure factor can be written in the form:

$$S_{\mathrm{inc}}(\boldsymbol{q},\omega) = R(\boldsymbol{q}) \otimes \left\{ \exp\left(-\frac{\hbar\omega}{2kT}\right) \exp(-\langle u^2\rangle q^2)[A_0(\boldsymbol{q})\delta(\omega) + \sum_i A_i L(\Gamma_i, \omega)] + U \right\} \quad (1)$$

where $R(\boldsymbol{q})$ is the resolution function of the instrument, A_0

is the amplitude of the EISF, A_i is the amplitude of the Lorentzian function, $L(\Gamma_i,\omega)$ is the Lorentzian line shape function with the line width Γ_i, and U is the background. According to this representation, the EISF is defined as the ratio of the elastic fraction of the amplitude to the total amplitude, with the sum of the amplitudes normalized to 1.

The first exponential in eq 1 is called the detailed balance factor (DBF) which takes into account the asymmetry of the density of states due to the Boltzmann distribution. Since the transfer energy is small compared to the thermal energy, the DBF is approximately unity. The second exponential is the Debye−Waller factor (DWF), by which the experimental dynamic structure factor has to be divided to obtain correct intensities. It arises from fast intramolecular vibrations exceeding the frequency window of the instrument, and reduces the signal with q^2, where $<u^2>$ in eq 1 is the mean squared amplitude of the vibration. It was determined for the IN5 instrument by measuring the total integrated intensity as a function of $\boldsymbol{q}$. From the slope of the plot ln $[I(\boldsymbol{q},t)]$ vs q^2, we obtained $<u^2> = 0.1 \pm 0.03$ Å^2.

Our experimental work employed the IN10/IN16 and IN13 backscattering spectrometers and the IN5 time-of-flight spectrometer at the Institute Max von Laue−Paul Langevin (Grenoble, France). The backscattering spectrometer was used in the configuration IN10a [energy analysis by unpolished Si(111) crystals], with an incident wavelength of 0.6271 nm and an energy resolution of 1 μeV (8 μeV for IN13). The time-of-flight IN5 spectrometer, where the energy analysis is simply done by measuring the flight time of the neutrons from sample to detector, was used at an incident wavelength of 1.0 nm, giving an energy resolution of 14.0 μeV. For the IN13 measurements, the instrument resolution was set to 8 μeV, the energy window covered the range −50 to 50 μeV, and the q range studied was 1.2−5.5 Å^{-1}. Since the flux on IN13 was quite low and the objective of these experiments was the verification of the models fitted to the EISF, experiments on IN13 were carried out using the fixed window technique with the center of the window at $\Delta E = 0$ μeV. This technique yields the scattering which is detected within the elastic resolution function of the instrument, and includes motions with frequencies modulated by the Debye−Waller factor. Thus, no motional correlation times could be extracted from the IN13 measurements.

To measure the anisotropy of sterol motion and take full advantage of the use of oriented multilayer samples, two orientations of the sample in the neutron beam were measured. The scattering geometry is schematically depicted in Figure 2. At an orientation of 135° between the incident neutron beam and the membrane normal (=normal to the Si wafer), the momentum transfer is mainly directed perpendicular to the membrane normal [i.e., parallel to the bilayer plane ($x-y$ plane)]. In this case, the in-plane (lateral) motion of the sterol under study will dominate the incoherent scattering. On the other hand, at an orientation of 45° the momentum transfer is mainly parallel to the membrane normal, and thus the incoherent scattering is dominated by out-of-plane (transverse) motion of the sterol along the z-direction (=membrane normal). QENS measurements were carried out at three temperatures: below and above the liquid−gel phase transition of pure DPPC-d_{75} (37 °C) at 20 and 50 °C, respectively, and at the physiologically important temperature of 36 °C.

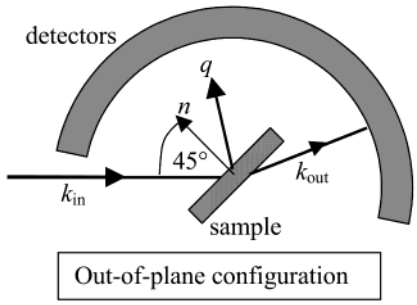

FIGURE 2: Schematic depiction of the QENS scattering geometry used for orientation-dependent measurements. The scattering angle between the incident neutron beam and the sample normal was 45° (135°), resulting in a momentum transfer directed predominantly parallel (perpendicular) to the sample normal.

Data Analysis and Reduction. Interpretation of the data was performed by use of Bayesian analysis (*20*) in terms of previously established cholesterol motional models (*15*). In a first step, the line shape parameters A_0, A_i, and Γ_i were fitted to each spectrum separately according to eq 1 and using a fixed DWF. From these parameters, the EISF and QISF were calculated. In a second step, the motional models have been fitted to the parameters simultaneously for all q values. It should be emphasized that all calculations for the models take into account the deviations of the different $\boldsymbol{q}$ vectors from the perpendicular and the parallel vector. Since we were mainly interested in a direct comparison of the three samples, the data sets of all three samples were analyzed by the same set of motional models. For brevity, we restrict our description of the models used, and point to the references given below concerning details of the calculations.

(i) Since the QENS spectra at this energy resolution are dominated by translational diffusion of the whole molecules (*16, 21*), we first analyzed the QENS spectral line widths $\Gamma(\boldsymbol{q})$ in terms of long-range diffusion of the sterols. This was achieved by fitting the QENS spectra by a single quasi-elastic (Lorentzian) line, as is typical for the case of Fickean diffusion (*19*). For the FWHM of the Lorentzian, $\Gamma(\boldsymbol{q})$, the Fickean theory predicts a linear dependence of $\Gamma(\boldsymbol{q})$ vs q^2 with the slope D (long-range diffusion coefficient) in the limit of small q (i.e., large distances).

(ii) However, it is known that for large values of the momentum transfer, details of the motion over short distances require a modification of Fick's law (*19*). This is usually taken into account by the use of jump diffusion models. The scattering law for anisotropic self-diffusion in liquid crystals calculated by Rosciszewski (*22*) was selected as the most appropriate jump diffusion model for the analysis of our data.

(iii) In-plane motion was considered by a composite model consisting of jump motion over a mean jump distance d at a jump rate $1/\tau$, and a continuous rotational diffusion (*19, 23*) about the sterol long axis (z-axis, normal to the bilayer) with a mean radius r. This model was previously applied to analyze cholesterol rotation (*15*). Finally for sterol motion along the membrane normal (out-of-plane or transverse motion), we employed a model of two-site jump diffusion (*19*) with spatial extent d_z and jump rate $1/\tau_z$. In cases where the jump diffusion model alone provided an unsatisfactory fit of the EISF, this model was superimposed by a spatially restricted diffusion (*19, 24*) of the sterol over a distance d_{1d}.

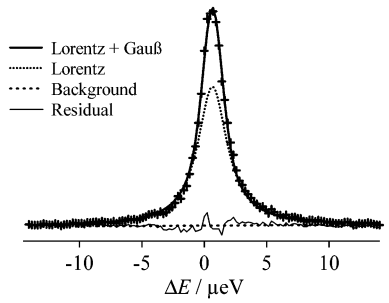

FIGURE 3: Representative QENS spectrum (IN10) of 40 mol % cholesterol in an oriented DPPC-d_{75} bilayer stack at a temperature of 50 °C. The experimental errors correspond approximately to the size of the data points. The fit to the data (crosses) consists of three parts: linear background (dashed line), quasi-elastic line (dotted Lorentzian), and the EISF (Gaussian; in this representation the solid line is a superposition of all three components). The spectrum was measured at $q = 1.41$ Å^{-1} at an orientation of the sample normal relative to the incident neutron beam of 45°, probing the out-of-plane motion. The thin solid line shows the residual of the fit.

This composite model was previously successfully applied to lipid motion (*21*).

RESULTS

The sterol dynamics in DPPC-d_{75} oriented bilayers were measured at three partially overlapping frequency regimes determined by the energy resolution of the QENS instrument. Correspondingly, the fast lipid dynamics were studied at a low resolution of $\Gamma = 14$ μeV using the time-of-flight IN5 spectrometer, while motions having longer correlation times were detected by the backscattering spectrometer IN10 operating at $\Gamma = 1$ μeV. Between these two resolutions, we employed the IN13 spectrometer at $\Gamma = 8$ μeV, but at a q range more than twice as wide than for the other two spectrometers. These various energy resolutions have been demonstrated previously to allow a comprehensive description of lipid (*21*, *25*) and of sterol motions (*15*), covering the range from fast rotational motion of the sterols at high frequencies (upper GHz range) to lateral lipid diffusion at the low-frequency side (lower GHz range). Furthermore, all measurements were done at two orientations of the sample normal (=normal direction of the oriented lipid multilayers) with respect to the incident neutron beam (Figure 2). Experiments performed at the 135° orientation essentially detected sterol motions in the plane of the bilayer such as lateral diffusion, while those conducted at 45° had the momentum transfer mainly directed along the membrane normal, and thus were sensitive to the out-of-plane sterol motion.

Quasi-elastic Neutron Scattering Measurements. As an example, Figure 3 shows a typical QENS spectrum (energy representation) measured using the backscattering instrument IN10. Results are depicted for cholesterol in a liquid-ordered (lo) DPPC-d_{75} bilayer at 50 °C for the 45° orientation ($q = 1.41$ Å^{-1}). The separation of the data into a Lorentzian and a Gaussian part is shown by the dashed and dotted lines, giving the relative amplitudes of the elastic (EISF = amplitude of the resolution function/total amplitude) and inelastic (QISF = amplitude of the Lorentzian/total amplitude) parts, respectively, along with the line width of the latter.

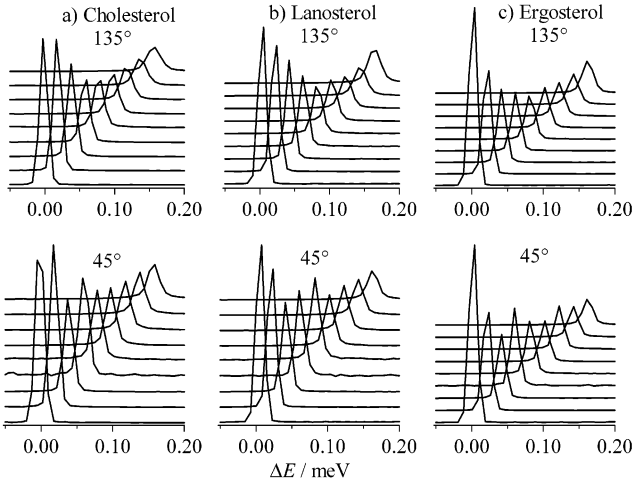

FIGURE 4: Time-of-flight instrument IN5: QENS spectra of 40 mol % (a) cholesterol, (b) lanosterol, and (c) ergosterol in a DPPC-d_{75} oriented bilayer stack at 36°C, measured with the sample normal oriented at 135° (top) and at 45° (bottom) relative to the incident neutron beam. The spectra are presented from left to right in order of increasing momentum transfer q, ranging from 0.17 to 1.07 Å^{-1}.

QENS spectra were obtained for bilayers of DPPC-d_{75} containing 40 mol % of cholesterol, lanosterol, or ergosterol with the IN5, IN13, and IN10 spectrometers at temperatures of 20, 36, and 50 °C. Figure 4 (a)−(c) shows representative sets of QENS spectra obtained using the time-of-flight IN5 spectrometer for bilayers of DPPC-d_{75} containing cholesterol, lanosterol, or ergosterol (6:4 molar ratio) at 36 °C. In the top row, the QENS spectra are plotted as a function of the momentum transfer q for the 135° bilayer orientation relative to the incident neutron beam (in-plane direction), and in the bottom row for the 45° orientation (out-of plane direction). As can be seen, changes in the apparent peak heights and widths occur as a function of the wavenumber q, which are further interpreted below. Similar results were obtained at 20 and 50 °C (not shown).

Figure 5 shows a representative analysis and reduction of QENS data acquired with the time-of-flight IN5 spectrometer (energy resolution 14.0 μeV; q range of 0.17−1.07 Å^{-1}), for DPPC-d_{75}/cholesterol (6:4) bilayers at several different temperatures. The corresponding data for DPPC-d_{75} containing 40 mol % of lanosterol or ergosterol were similarly reduced and analyzed (not shown). The elastic incoherent structure factor (EISF) is shown in Figure 5(a),(b) for the in-plane (135°) and out-of-plane (45°) orientations, respectively, and is seen to decrease with increasing q. The Lorentzian full width at half-maximum (FHWM) of the quasi-elastic line as shown in Figure 5(c),(d) for the 135° and 45° orientations increases with q. The models (i)−(iii) were fitted to the data (cf. Materials and Methods) as discussed below.

An analysis of the QENS results using the IN13 backscattering spectrometer (energy resolution 8 μeV; q range 1.2−5.5 Å^{-1}) for DPPC-d_{75}/cholesterol (6:4) bilayers is presented in Figure 6. Parts (a) and (b) show the data for the 135° orientation (in-plane) and 45° orientation (out-of-plane), respectively. Here the extended q range is proved most useful in further testing models for the structural fluctuations (vide infra). However, the neutron flux of the IN13 instrument was too low in the quasi-elastic mode to obtain reasonable statistics within an acceptable acquisition

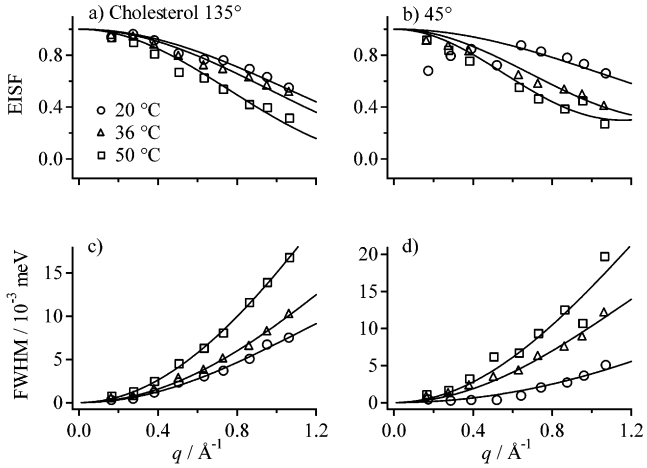

FIGURE 5: Time-of-flight instrument IN5 data analysis: (a) EISF versus q for bilayers of DPPC-d_{75} containing 40 mol % cholesterol having a 135° and (b) 45° orientation at temperatures of 20 °C (circles), 36 °C (triangles), and 50 °C (squares). The solid lines represent fits of the following composite models to the data: 135° orientation (lateral motion), continuous rotational diffusion; 45° orientation (transverse motion), two-site jumps. (c) Quasi-elastic line width (FWHM) vs q for DPPC-d_{75} bilayers containing 40 mol % cholesterol having a 135° and (d) 45° orientation at temperatures of 20 °C (circles), 36 °C (triangles), and 50 °C (squares). The full lines represent fits of the data to the models which give the lateral (135°) or transverse (45°) motional rates (cf. text).

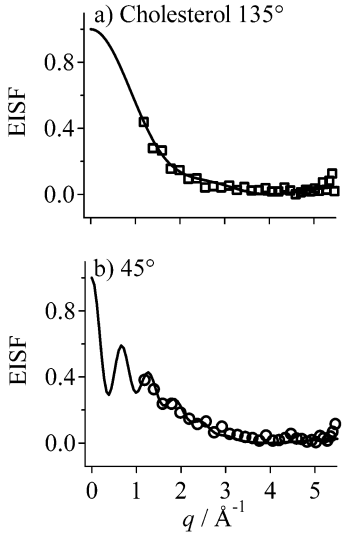

FIGURE 6: Backscattering instrument IN13 data analysis: (a) EISF versus q for bilayers of DPPC-d_{75} containing 40 mol % cholesterol at 36 °C for orientations of 135° and (b) 45°. The solid lines represent fits of the following composite models to the data: 135° orientation (lateral motion), continuous rotational diffusion, superimposed with two-site jumps when necessary; 45° orientation (transverse motion), two-site jumps, superimposed with a local one-dimensional diffusion.

time. Therefore, we concentrated solely on the measurement of the signal around $\Delta E = 0$ μeV by choosing the fixed window mode. Figure 6 illustrates clearly that the EISF for both orientations, parts (a) and (b), decays to zero by about $q = 3.5$ Å^{-1}. The same set of theoretical models was used to fit the data as for the IN10 data (below). The corresponding IN13 experiments for the bilayers of DPPC-d_{75} containing either lanosterol or ergosterol (6:4) were not carried out, owing to beam time restrictions.

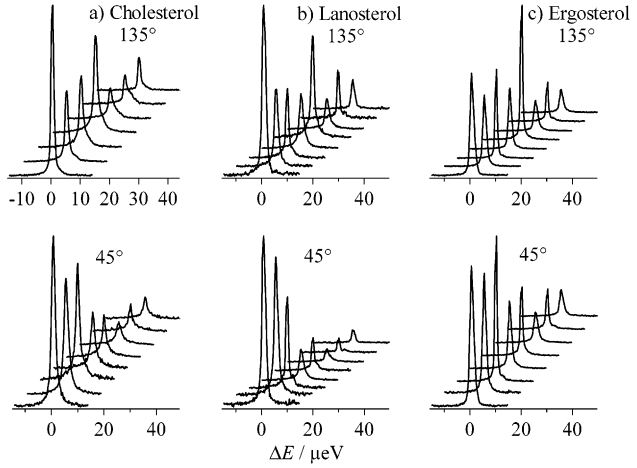

FIGURE 7: Backscattering instrument IN10: QENS spectra of 40 mol % (a) cholesterol, (b) lanosterol, and (c) ergosterol in a DPPC-d_{75} oriented bilayer stack at 36°C. The spectra were measured with the sample normal aligned relative to the incident neutron beam at 135° (top) and at 45° (bottom), and are shown from left to right in order of increasing momentum transfer q, ranging from 0.41 to 1.95 Å^{-1}.

Figure 7 (a)−(c) depicts representative QENS spectra acquired for DPPC-d_{75} bilayers containing cholesterol, lanosterol, or ergosterol (6:4 molar ratio), respectively, using the IN10 backscattering spectrometer (energy resolution 1 μeV; q range 0.41−1.95 Å^{-1}) at 36 °C. The top row indicates spectra for the 135° orientation (in-plane momentum transfer) as a function of q, and the bottom row shows the corresponding data for the 45° orientation (out-of-plane momentum transfer). In each case, the QENS spectra exhibit characteristic peaks and changes in apparent line width as a function of q. Similar results were obtained for each of the three systems at temperatures of 20 and 50 °C (not shown).

Finally, the analysis of representative QENS data for DPPC-d_{75}/cholesterol (6:4) bilayers is shown in Figure 8 for the case of the IN10 backscattering spectrometer at the various temperatures. The EISF in Figure 8(a),(b) for the in-plane (135°) and out-of-plane (45°) scattering is found to decrease with several peaks resolved in part (a). The FWHM of the quasi-elastic line shows a broad maximum with increasing q over the measured range of the momentum transfer. Data for DPPC-d_{75} containing either lanosterol or ergosterol were similarly analyzed and interpreted (not shown).

Data Fits to Theoretical QENS Spectra. For the bilayers of DPPC-d_{75} containing cholesterol, lanosterol, or ergosterol (6:4), the QENS data at each of the three temperatures (20, 36, 50 °C) were analyzed in terms of models (i)−(iii) as described above. The results of the fitting procedure are summarized in Tables 1−3.

Data analysis in terms of the long-range diffusion model (i) (cf. Materials and Methods) revealed major differences in the diffusive behavior of the three sterols. The D values extracted from the model fits to the line widths of the IN10 quasi-elastic spectra (e.g., as shown for cholesterol in Figure 8, bottom) are summarized in Table 1 for the two sample orientations and three different temperatures. At low temperature (20 °C), cholesterol showed a factor of 4 higher transverse diffusion coefficient D_t than ergosterol, with lanosterol diffusion in between. In the lateral direction, both

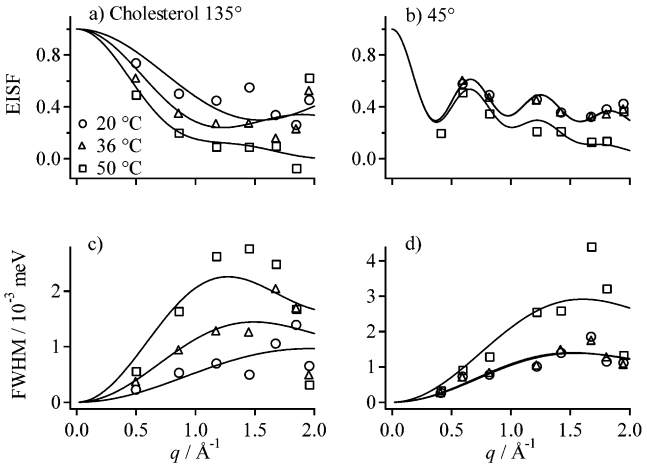

FIGURE 8: Backscattering instrument IN10 data analysis: (a) Elastic incoherent structure factor (EISF) versus q for DPPC-d_{75} bilayers containing 40 mol % cholesterol having a 135° and (b) 45° orientation at temperatures of 20 °C (circles), 36 °C (triangles), and 50 °C (squares). The solid lines represent fits to the data using the same set of models as for the IN13 data. (c) Quasi-elastic line width (FWHM) vs q for DPPC-d_{75} bilayers containing 40 mol % cholesterol having a 135° and (d) 45° orientation at temperatures of 20 °C (circles), 36 °C (triangles), and 50 °C (squares). The full lines represent fits of the data to a continuous diffusion model which gives the lateral (135°) or transverse (45°) long-range diffusion constant D (cf. text).

Table 1: Long-Range Diffusion Constants D in the Transverse (Out-of-Plane) and Lateral (In-Plane) Directions Obtained from IN10 (Lower Frequency) Measurements for the Three Sterols in DPPC-d_{75} at Three (Two) Temperatures

$D/10^{-12}$ m^2 s^{-1} at		6:4 DPPC/ cholesterol	6:4 DPPC/ lanosterol	6:4 DPPC/ ergosterol
20 °C	lateral	5.2 ± 2.3	6.7 ± 1.2	1.8 ± 1.6
	transverse	23.5 ± 3.8	13.5 ± 3.3	5.9 ± 3.4
36 °C	lateral	13.5 ± 3.6	17.9 ± 2.5	3.5 ± 1.5
	transverse	24.6 ± 3.9	30.5 ± 6.6	9.5 ± 2.5
50 °C	lateral	30.3 ± 6.6	−	9.5 ± 1.2
	transverse	47.8 ± 12.3	−	18.6 ± 3.0

cholesterol and lanosterol diffusion D_l was a factor of ~3 higher than for ergosterol. Consequently, the largest diffusional anisotropy $D_a = D_t/D_l$ was obtained for cholesterol ($D_a = 4.5$), while ergosterol ($D_a = 3.2$) and lanosterol ($D_a = 2.0$) gave significantly lower anisotropies. A temperature increase caused for all three sterols an increase of the lateral diffusion rate, with the most pronounced effect for cholesterol and lanosterol (D_l approximately tripled for each 15 °C temperature increase), while the increase in the transverse diffusion rate was less significant. Hence, the anisotropy D_a was lower for cholesterol ($D_a = 1.6$) compared to ergosterol ($D_a = 2.0$) at 50 °C.

It was shown previously that the IN5 time window is not suitable for long-range diffusion measurements (*21, 25*) owing to the sensitivity of this instrument for motions with shorter correlation times. Nevertheless, the IN5 data provided a similar anisotropy of the sterol motion and temperature dependencies as obtained for IN10.

Further analysis of the EISF and the quasi-elastic line width Γ of the spectra in terms of the composite motional models (cf. Materials and Methods) provided more detailed information about the geometry and correlation times of the sterol motions in the bilayer. The data in Figures 5, 6, and 8 show as an example the 40 mol % cholesterol/DPPC-d_{75} bilayers measured using the IN5, IN13, and IN10 spectrometers, along with the fits to the composite model as described in the data analysis section above. The data for the DPPC-d_{75} bilayers containing lanosterol or ergosterol were analyzed similarly. The results are summarized in Table 2 for lateral motion [135° orientation, model (ii)] and in Table 3 for transverse motion [45° orientation, model (iii)].

Table 2: Results Obtained from QENS Spectra (IN5, IN13, and IN10) for Lateral Sterol Motion in DPPC-d_{75} (135° Orientation)[a]

		6:4 DPPC/ cholesterol	6:4 DPPC/ lanosterol	6:4 DPPC/ ergosterol
IN5				
20 °C	r/Å	1.01 ± 0.02	0.87 ± 0.01	0.77 ± 0.01
	$D_r/10^{10}$ rad^2 s^{-1}	2.4 ± 0.2	2.4 ± 0.1	2.9 ± 0.1
36 °C	r/Å	1.12 ± 0.02	1.13 ± 0.01	0.89 ± 0.01
	$D_r/10^{10}$ rad^2 s^{-1}	2.8 ± 0.1	2.6 ± 0.1	2.6 ± 0.1
50 °C	r/Å	1.42 ± 0.02	−	1.08 ± 0.01
	$D_r/10^{10}$ rad^2 s^{-1}	2.51 ± 0.09	−	2.75 ± 0.09
IN13				
36 °C	r/Å	0.60 ± 0.01	−	−
	d/Å	1.80 ± 0.05	−	−
IN10				
20 °C	r/Å	−	−	−
	d/Å	2.48 ± 0.03	1.94 ± 0.05	1.12 ± 0.01
	$\tau/10^{-9}$ s	1.05 ± 0.03	0.86 ± 0.04	8 ± 1
36 °C	r/Å	0.54 ± 0.02	0.25 ± 0.03	−
	d/Å	3.26 ± 0.04	3.25 ± 0.04	1.43 ± 0.02
	$\tau/10^{-9}$ s	1.00 ± 0.02	1.01 ± 0.03	1.53 ± 0.07
50 °C	r/Å	1.11 ± 0.02	−	0.16 ± 0.05
	d/Å	3.78 ± 0.08	−	2.85 ± 0.03
	$\tau/10^{-9}$ s	0.87 ± 0.02	−	1.03 ± 0.03

[a] The model employed for this orientation was a continuous rotational diffusion of radius r and diffusion constant D_r, superimposed, if required, for IN10 and IN13 data, by a two-site jump of amplitude d and jump rate $1/\tau$.

Table 3: Results Obtained from QENS Spectra (IN5, IN13, and IN10) for Transverse Sterol Motion in DPPC-d_{75} (45° Orientation)[a]

		6:4 DPPC/ cholesterol	6:4 DPPC/ lanosterol	6:4 DPPC/ ergosterol
IN5				
20 °C	d_z/Å	1.75 ± 0.02	2.05 ± 0.02	1.64 ± 0.02
	$\tau_z/10^{-11}$ s	6.6 ± 0.4	13.6 ± 0.6	7.8 ± 0.4
36 °C	d_z/Å	2.67 ± 0.03	2.91 ± 0.04	1.99 ± 0.02
	$\tau_z/10^{-11}$ s	9.2 ± 0.3	8.2 ± 0.3	7.6 ± 0.3
50 °C	d_z/Å	3.31 ± 0.05	−	2.49 ± 0.03
	$\tau_z/10^{-11}$ s	8.3 ± 0.3	−	7.2 ± 0.2
IN13				
36 °C	d_z/Å	10.3 ± 0.1	−	−
	d_{1d}/Å	1.59 ± 0.02	−	−
IN10				
20 °C	d_z/Å	10.5 ± 0.1	2.37 ± 0.04	1.26 ± 0.01
	$\tau_z/10^{-9}$ s	0.55 ± 0.02	1.18 ± 0.06	17 ± 2
	d_{1d}/Å	1.25 ± 0.03	−	−
36 °C	d_z/Å	10.5 ± 0.1	3.11 ± 0.05	1.61 ± 0.02
	$\tau_z/10^{-9}$ s	0.47 ± 0.02	0.72 ± 0.03	3.6 ± 0.2
	d_{1d}/Å	1.25 ± 0.03	0.72 ± 0.08	−
50 °C	d_z/Å	10.4 ± 0.1	−	2.60 ± 0.02
	$\tau_z/10^{-9}$ s	0.53 ± 0.02	−	2.15 ± 0.09
	d_{1d}/Å	2.26 ± 0.04	−	−

[a] The model employed was a two-site jump of amplitude d_z with jump rate $1/\tau_z$, superimposed, if required for IN10 and IN13 data, with a one-dimensional local diffusion of amplitude d_{1d}.

Considering first the results for lateral motion (Table 2), the rotational diffusion as measured by the IN5 spectrometer is the most interesting parameter, since this energy resolution (14 μeV) is most sensitive for correlation times typical of

molecular rotations. The rotational diffusion constants D_r (Table 2, IN5 results) do not indicate significant differences for the three sterols; however, cholesterol clearly required the largest rotational radius at all three temperatures. The correlation times τ of the lateral diffusion jump rate as measured by the IN10 and IN13 spectrometers show a weak temperature dependence for cholesterol and lanosterol, whereas ergosterol gave a remarkably high value at 20 °C. The fact that the IN5 fitting results (as shown for cholesterol in Figure 4 and summarized in Tables 2 and 3) showed no significant differences between the transverse spatial extent of the motion is not surprising: The shorter time scale of this experiment does not allow the observation of motion over distances of more than 1−2 Å. The jump rates $1/\tau_z$ were only slightly temperature-dependent for cholesterol and lanosterol, whereas this rate changed by nearly an order of magnitude for ergosterol, with the smallest jump rate at 20 °C (IN10 results, Table 3).

As the q range of both the IN5 and IN10 spectrometers was insufficient to allow the EISF to decrease down to zero, we used the IN13 spectrometer with its extended q range to verify the cholesterol/DPPC measurements, and thus to further justify the choice of the models used for data analysis. Figure 6 clearly shows that the EISF for both orientations goes down to zero at about $q = 3.5$ Å^{-1}. The same set of models was used for fitting the EISF (solid lines) as for the IN10 data. The results for the lateral and transverse motion (Tables 2 and 3) are indeed very similar to those obtained by the other instruments, providing additional strong support for the choice of models applied in the data analysis. The most striking result is the drastic difference in the spatial extensions d_z of the transverse sterol motion (Table 3). Here we obtained for the IN10 data for all temperatures a spatial extent of $d_z > 1.0$ nm for cholesterol, whereas the other two sterols showed a d_z of 0.3 nm and less. It is noteworthy that the high spatial extension of cholesterol transverse motion was confirmed in the independent IN13 measurement, in which the q range was extended by a factor of 2 (as compared to IN10) and allowed a higher fidelity fit to the model (see above).

The data analysis summarized in Tables 2 and 3 allows us to conclude that the truly significant differences in the motion of the three sterols are in the out-of-plane (transverse) direction, while the in-plane (lateral) motion is rather similar for the three molecules. To appreciate this, it should be emphasized that for all three sterols the same set of motional models has been used.

DISCUSSION

The focus of this work is a comparative study of the molecular dynamics of sterols in lecithin bilayers. The above results strongly suggest that cholesterol has the most unusual molecular dynamics of the three sterols: it showed the largest motional anisotropy D_a of translational long-range diffusion at low temperature (20 °C), and the strongest temperature dependence of D_a for all three sterols ($D_a = 4.5$ at 20 °C and $D_a = 1.6$ at 50 °C). Moreover, its amplitude of transverse (out-of-plane) motion was at least a factor of 3 larger than for the two other sterols, independent of temperature. In contrast, ergosterol showed the slowest motion in all respects: its transverse diffusion was a factor of 2−3 lower than for cholesterol and lanosterol, and only slightly temperature-dependent. Its lateral motion as seen by the IN10 spectrometer was a factor of 4−5 slower than for the other two molecules, while the temperature dependence of this lateral diffusion was comparable to the other sterols. Moreover, the spatial extent of its transverse motion did not exceed a maximum value of 0.25 nm, thus being a factor of 4−5 less (depending on temperature) than for cholesterol. Finally, ergosterol also showed the lowest radius for rotational motion with respect to the membrane normal.

The most obvious reason for these significant variations in sterol molecular dynamics comes from their structural differences (*26*−*28*) despite their similar overall length derived from the crystal structures (C_3 to C_{25} distances of 14.9 Å for cholesterol, 14.3 Å for lanosterol, and 14.7 Å for ergosterol). Cholesterol and ergosterol show a similar sterol frame with one side being rather flat but have differently structured alkyl chains (Figure 1), suggesting a crucial effect of the alkyl chain on the molecular dynamics of these sterols. Ergosterol, in comparison to cholesterol, features an additional double bond and methyl group in this chain. This may increase the cross section of this chain beyond the limits of the sterol body cross section (in particular along the sterol body normal direction), giving the chain a much stronger interaction potential with the surrounding DPPC chains (*26*, *29*, *30*). This is also indicated by the fact that DPPC chains adopt a significantly higher molecular order in the presence of 40 mol % ergosterol as compared to the same amount of cholesterol (*31*). As a result, the ergosterol alkyl chain interaction with the lipid chains may be an efficient way to dissipate thermal energy, thereby rendering the molecule less mobile within the lipid environment than in the case of cholesterol. For the latter sterol, we have already provided a rationale for its high-amplitude transverse motion in a previous QENS paper (*15*). There we suggested that a part of cholesterol, namely, its alkyl chain, may fluctuate at high frequencies into the opposite leaflet of the bilayer, giving rise to a dynamically rough boundary between the two monolayers of the membrane. The bulkier alkyl chain of ergosterol may prevent such motions by higher molecular friction and/or repulsion from the opposite monolayer, and thus maintain the transverse amplitude in the same range as was previously observed for pure DPPC (*25*) in fully hydrated bilayer stacks.

The significantly slower lateral diffusion rate of ergosterol compared to cholesterol (a factor of 3−4 depending on temperature; cf. Tables 1 and 3) can be explained in a similar way. Since ergosterol is bulkier in a region close to the bilayer center, where usually the lipids exhibit lowest molecular order, this molecule will reduce the fluidity [as evident from the increase of lipid chain order parameter, cf. (*31*)] in this region, and thus decrease the lateral diffusion rate.

With the exception of a double bond, lanosterol exhibits the same alkyl chain as cholesterol, but a much bulkier sterol frame owing to the three additional methyl groups. In this case, the site of strongest interaction with the surrounding lipid chains can be expected to be shifted away from the bilayer center toward the interface. Thus, lanosterol cannot impose as high a molecular order to the lipid chains, and NMR experiments showed that indeed this order parameter is lower than for the other two sterols (*31*). Consequently,

lanosterol is unlikely to exhibit large amplitudes for transverse motion, as the friction between its bulky sterol body and the lipid chains will dissipate thermal energy efficiently. There is also a steric argument why this sterol cannot, like cholesterol, penetrate with its alkyl chain into the opposite monolayer. Its effective molecular barrel-like shape will enable the terminal groups of the adjacent lipid chains to adopt a rather low order; i.e., a high number of kinks is likely to occur there (*29*), which is also reflected in the acyl chain packing. These disordered segments will effectively overdamp the transverse sterol motion toward the bilayer center and beyond. At the same time, this low order will allow for a rather fast lateral diffusion of lanosterol (*26*). As can be inferred from Table 1, this sterol indeed showed the fastest motion in this direction. To sum up, only cholesterol is able to fluctuate over larger distances (1 nm) in the transverse direction, and thus provide a dynamically rough interface between the two monolayer leaflets at the bilayer center, whereas both lanosterol and ergosterol remain largely confined to their host monolayer.

Several papers of our group have suggested the possibility of hydrogen bonding between the cholesterol hydroxyl group and the oxygen of the glycerol backbone of the lipid (*28, 32*−*35*). The definition of a hydrogen bond after Raghaven (*33*) is given by (i) a distance between the oxygen in the lipid glycerol backbone and the oxygen of the cholesterol of less than 3.25 Å and (ii) an angle between the vector oxygen(lipid)−oxygen(cholesterol) and the vector of the cholesterol OH-bond of less than 35°. According to our results, a hydrogen bond could indeed exist within the characteristic time τ_z of the jump rate, which is about 0.5 ns (Table 2). Tu et al. have observed a distribution of the cholesterol hydroxyl position of about 6 Å between the carbonyl and the choline of the lipid (*36*). Moreover, NMR data suggest that cholesterol rotates similarly to the phopholipids, and thus is unable to bind to the lipid more permanently in a specific manner (*12, 37*−*39*).

The influence of the three sterols on the bilayer can be further discussed in terms of their hydrophobic length match with the DPPC alkyl chains. The above-mentioned structural features of cholesterol might lead to a mismatch of the projected hydrophobic length of cholesterol versus the interacting DPPC molecules, requiring that the alkyl chain of cholesterol penetrates more deeply into the apposed monolayer leaflet of the bilayer, leading to a large influence on the acyl chain conformational ordering. By contrast, we propose that lanosterol and ergosterol have a closer hydrophobic match to the interacting DPPC molecules, but for different reasons. In the case of lanosterol, the presence of the two additional methyl groups on the α-face, together with the steric hindrance provided by the additional double bond at the end of the alkyl tail, may result in a matching of the average hydrophobic lengths with only minimal penetration or interdigitation into the apposing monolayer leaflet. Ergosterol differs from the structure of cholesterol by an additional double bond in the sterol frame and the alkyl tail and the presence of a third methyl group at the end of the tail. In this case, the steric hindrance may also lead to a change in the hydrophobic length of the ergosterol molecule, thus matching the interacting DPPC molecule without requiring penetration of the opposing monolayer.

Moreover, fluctuations of the sterols into the headgroup region or beyond into the aqueous bulk are unlikely to occur due to the energy balance. Previous ^{2}H NMR studies have indicated that cholesterol acts as a spacer molecule, and does not greatly perturb the lipid polar headgroups (*40*). For example, the estimated energy for the protrusion of a CH_2-group into the aqueous phase is about $(5-6) \times 10^{-21}$ J·m^{-1}, while the thermal energy is only about $(3-5) \times 10^{-21}$ J·m^{-1} (*21*). However, toward the bilayer midplane, sufficient free volume exists due to the fluctuations of the lipid chains. The rigid sterol body and the fact that over 80% of the cholesterol side chain favor the all-trans configuration will facilitate motions in the transverse direction (*36, 41*). Worcester et al. (*42*) measured by neutron diffraction the distribution of the deuterium-labeled C_3 position of cholesterol in a 6:4 egg-lecithin/cholesterol mixture. They found two peaks separated by a distance of 17.5 Å, each having a full width at half-maximum of 4.5 Å. Unfortunately, these authors did not discuss the smaller two peaks in their paper, which have about the same FWHM and a distance of 3.5 Å from the bilayer midplane. In the context of our data analysis, this observation suggests that the peaks arise from cholesterol molecules fluctuating into the opposite bilayer leaflet.

It is interesting to note that in a recent molecular dynamics simulation of a 6:4 DPPC/cholesterol system (unpublished), we observed that the center-of-mass trajectories of the cholesterol molecules showed a similar composite motional behavior as measured by QENS. To date, there has not been a comparison with the results of other groups in the field of molecular dynamics, regarding the center-of-mass trajectories of cholesterol. Early molecular dynamics simulations concentrated on pure lipid model systems, which have improved rapidly. For example, the work of Moore et al. (*43*) agrees well with our previous QENS work on pure PC bilayers (*21, 25*). Although several excellent MD simulations of lipid/cholesterol systems have been published over the past decade, their data analysis was largely restricted to the order parameter profiles of the lipid chains, the interaction of lipids and cholesterol (e.g., the phase diagram or the hydrogen bonding), and the tilt angles of the cholesterol molecules (*28, 34*−*36, 44, 45*). Smondyrev and Berkowitz (*28*) published lateral and transverse diffusion constants, but did not analyze the cholesterol trajectories for specific motional models, nor did other groups.

In a previous work (*31*) we observed strong correlations between the molecular ordering and NMR relaxation on one side, and the micromechanical properties of the sterol-doped DPPC bilayer on the other side. For example, the area expansion modulus, which also provides a measure of membrane bending stiffness (*10*), was found to be highest for ergosterol and lowest for lanosterol, with cholesterol between but closer to lanosterol. It is now tempting to search for connections between these properties and the molecular dynamics by comparison to the QENS results. Bending of the bilayer in general results in a loss of conformational entropy of the acyl chains, which is largest for the highly ordered ergosterol-containing bilayers, leading to a larger bending rigidity than for cholesterol and even more compared to lanosterol. We may assume that the amplitude of transverse motion and the anisotropy D_a are relevant parameters for these properties. It follows that ergosterol with its generally low values of these parameters may be an

example for the creation of very stiff and less flexible membranes. On the other hand, cholesterol and to some extend lanosterol would serve as membrane fluidizers (*46*, *47*), but with the unique option that cholesterol can additionally create a dynamically rough boundary at the bilayer center, thus rendering the membrane more robust and thus allowing for larger but still very soft membrane structures.

CONCLUSIONS

The QENS data suggest that modifications of the sterol frame as in the case of lanosterol, and changes of the sterol alkyl chain as for lanosterol and ergosterol, have a drastic effect on the molecular dynamics of these molecules in lecithin bilayers. The results may shed some light on the demise of lanosterol and the rise of cholesterol in the course of cellular evolution at the occurrence of the first metazoa. As already suggested by Bloch (*18*) and Bloom (*48*), lanosterol may have been unable to provide sufficiently stable bilayers to allow for larger and highly protein-containing membranes. The QENS data now furnish a reasoning for this failure in terms of its molecular dynamics. It seems that nature coped with this problem by shedding the three methyl groups from the lanosterol sterol body (this took about 1.5 eons, 1 eon $= 10^9$ years) to end up with cholesterol. The dynamically rough borderline at the bilayer center created by cholesterol and the high-temperature sensitivity of the composite bilayer may provide the flexible and soft matrix required for optimum activity of complex proteins, and a membrane stability allowing for larger (eukaryotic) cells.

REFERENCES

1. Finegold, L. (1993) *Cholesterol in Membrane Models*, 1st ed., CRC Press, Boca Raton, FL.
2. Simons, K., and Ikonen, E. (2000) *Science 290*, 1721−1726.
3. Brown, D. A., and London, E. (2000) *J. Biol. Chem. 275*, 17221−17224.
4. Radhakrishnan, A., Anderson, T. G., and McConnell, H. M. (2000) *Proc. Natl. Acad. Sci. U.S.A. 97*, 12422−12427.
5. Marx, J. (2001) *Science*, 1862−1865.
6. Ipsen, J. H., Karlström, G., Mouritsen, O. G., Wennerström, H., and Zuckermann, M. J. (1988) *Biochim. Biophys. Acta 905*, 162−172.
7. Vist, M. R., and Davis, J. H. (1990) *Biochemistry 29*, 451−464.
8. Nielsen, M., Thewalt, J., Miao, L., Ipsen, J. H., Bloom, M., Zuckermann, M. J., and Mouritsen, O. G. (2000) *Europhys. Lett. 52*, 368−374.
9. Miao, L., Nielsen, M., Thewalt, J., Ipsen, J. H., Bloom, M., Zuckermann, M. J., and Mouritsen, O. G. (2002) *Biophys. J. 82*, 1429−1444.
10. Evans, E., and Needham, D. (1986) *Faraday Discuss. Chem. Soc. 81*, 9999.
11. Evans, E., and Rawicz, W. (1990) *Phys. Rev. Lett. 64*, 2094−2097.
12. Brown, M. F. (1990) *Mol. Phys. 71*, 903−908.
13. Song, J. B., and Waugh, R. E. (1993) *Biophys. J. 64*, 1967−1970.
14. Brown, M. F., Thurmond, R. L., Dodd, S. W., Otten, D., and Beyer, K. (2001) *Phys. Rev. E 64*, 010901-1−010901-4.
15. Gliss, C., Randel, O., Casalta, H., Sackmann, E., Zorn, R., and Bayerl, T. (1999) *Biophy. J. 77*, 331−340.
16. König, S., Pfeiffer, W., Bayerl, T., Richter, D., and Sackmann, E. (1992) *J. Phys. (Paris) II 2*, 1589−1615.
17. Bloom, M., Morrison, C., Sternin, E., and Thewalt, J. L. (1992) in *Pulsed magnetic resonance: NMR, ESR and optics, a recognition of E. L. Hahn* (Bagguley, D. M. S., Ed.) pp 274−316, Clarendon Press, Oxford.
18. Bloch, K. (1985) *Cholesterol, evolution of structure and function*, Benjamin/Cummins, New York.
19. Bée, M. (1988) *Quasielastic Neutron Scattering. Principles and Applications in Solid State Chemistry, Biology and Materials Science*, Adam Hilger, Bristol and Philadelphia.
20. Sivia, D. S., Carlile, C. J., Howells, W. S., and König, S. (1992) *Physica B 182*, 341−348.
21. König, S., Bayerl, T. M., Coddens, G., Richter, D., and Sackmann, E. (1995) *Biophys. J. 68*, 1871−1880.
22. Rosciszewski, I. (1972) *Acta Phys. Pol., A 49*, 549.
23. Dianoux, A. J., Volino, F., and Hervert, H. (1975) *Mol. Phys. 30*, 1181−1194.
24. Hall, P. L., and Ross, D. K. (1978) *Mol. Phys. 36*, 1549−1554.
25. König, S., Pfeiffer, W., Bayerl, T., Richter, D., and Sackmann, E. (1992) *J. Phys. (France)*, 1589−1615.
26. Urbina, J. A., Pekerar, S., Le, H. B., Patterson, J., Montez, B., and Oldfield, E. (1995) *Biochim. Biophys. Acta 1238*, 163−176.
27. Nielsen, J. F., Zhang, R. T., Tristram-Nagle, S., Sun, W. J., Petrache, H. I., and Suter, R. M. (2000) *Biophys. J. 70*, 1419−1431.
28. Smondyrev, A. M., and Berkowitz, M. L. (2001) *Biophys. J. 80*, 1649−1658.
29. Yeagle, P. L. (1985) *Biochim. Biophys. Acta 815*, 33−36.
30. Singer, M. A., and Finegold, L. (1990) *Chem. Phys. Lipids 56*, 217−222.
31. Endress, E., Bayerl, S., Prechtel, K., Maier, C., Merkel, R., and Bayerl, T. M. (2002) *Langmuir* (in press).
32. Scott, H. L. (1991) *Biophys. J. 59*, 445−455.
33. Raghavan, K., Reddy, M. R., and Berkowitz, M. L. (1992) *Langmuir 8*, 233−240.
34. Pasenkiewicz-Gierula, M., Rog, T., Kitamura, K., and Kusumi, A. (2000) *Biophys. J. 78*, 1376−1389.
35. Chiu, S. W., Jakobsson, E., and Scott, H. L. (2001) *Biophys. J. 80*, 1104−1114.
36. Tu, K., Klein, M., and Tobias, D. (1998) *Biophys. J. 75*, 2147−2156.
37. Yeagle, P. L. (1981) *Biochim. Biophys. Acta 640*, 263−273.
38. Brown, M. F., and Nevzorov, A. A. (1999) *Colloids Surf., A 158*, 281−298.
39. Trouard, P. T., Nevzorov, A. A., Alam, T. M., Job, C., Zajicek, J., and Brown, M. F. (1999) *J. Chem. Phys. 110*, 8802−8818.
40. Brown, M. F., and Seelig, J. (1978) *Biochemistry 17*, 381−384.
41. Rohrer, A. J., Richards, W., Griffin, J., and Weeks, C. (1980) *Lipids 15*, 783−792.
42. Worcester, D. L., and Franks, N. P. (1976) *J. Mol. Biol. 100*, 359−378.
43. Moore, P. B., Lopez, C. F., and Klein, M. L. (2001) *Biophys. J. 81*, 2484−2494.
44. Scott, H. L., and Kalaskar, S. (1989) *Biochemistry 28*, 3687−3691.
45. Smondyrev, A. M., and Berkowitz, M. L. (1999) *Biophys. J. 77*, 2075−2089.
46. Presti, F. T., Aloia, R. C., and Boggs, J. M. (1985) *Cellular Aspects*, Vol. 4, pp 97−146, Academic Press, New York.
47. Yeagle, P. L. (1993) *The Membranes of Cells*, Academic Press, San Diego.
48. Bloom, M., and Mouritsen, O. G. (1988) *Can. J. Chem. 66*, 706−712.

BI0201670